ELSEVIER

www.elsevier.nl/locate/ica
Inorganica Chimica Acta 323 (2001) 119–129

Inorganica Chimica Acta

# Metal complexes as anticancer agents 2. Iron(III) and copper(II) bio-active complexes with $N^6$-benzylaminopurine derivatives

Michal Maloň [a], Zdeněk Trávníček [a,e,*], Miroslav Maryško [b], Radek Zbořil [c], Miroslav Mašláň [c], Jaromír Marek [d], Karel Doležal [e], Jakub Rolčík [e], Vladimír Kryštof [e], Miroslav Strnad [e]

[a] *Department of Inorganic and Physical Chemistry, Palacký University, Křížkovského 10, CZ-771 47 Olomouc, Czech Republic*
[b] *Institute of Physics ASCR, Cukrovarnická 10, CZ-162 53 Prague 6, Czech Republic*
[c] *Department of Experimental Physics, Palacký University, Tř. Svobody 26, CZ-771 46 Olomouc, Czech Republic*
[d] *X-ray Laboratory of Faculty of Science, Masaryk University, Kotlářská 2, CZ-611 37 Brno, Czech Republic*
[e] *Laboratory of Growth Regulators, Institute of Experimental Botany ASCR and Palacký University, Šlechtitelů 11, CZ-783 71 Olomouc, Czech Republic*

Received 5 March 2001; accepted 6 August 2001

**Abstract**

Iron(III) complexes with 2-(3-hydroxypropylamino)-6-benzylamino-9-isopropylpurine (*Bohemin*, $HL_1$), in its protonized form, of the composition $(H^+HL_1)_2[FeCl_5]\cdot 2H_2O$ (**1**), $(H^+HL_1)_2[FeCl_5]\cdot 3H_2O$ (**2**) have been prepared by two different routes. A new way for synthesis of copper(II) complex with 6-(2-chlorobenzylamino)purine ($HL_2$), $[Cu_2(\mu\text{-}Cl)_2(\mu\text{-}HL_2)_2(HL_2)_2Cl_2]\cdot 2H_2O$ (**3**), together with the preparation of copper(II) complex with 6-(3-chlorobenzylamino)purine ($HL_3$), $[Cu_2(\mu\text{-}Cl)_2(\mu\text{-}HL_3)_2Cl_2]$ (**4**), is also reported. The characterization have been based on elemental analysis, electronic, infrared, ES+ mass and $^{57}$Fe Mössbauer spectra, conductivity data and magnetic susceptibility temperature measurements over the 4.5–300 K for **1**–**3**, and 35–300 K for **4**, temperature range, respectively. Molecular structure of an electroneutral form of the $HL_2$ ligand, ($HL_2\cdot 2H_2O$), and a protonized form of the $HL_3$ ligand, ($H^+HL_3$–Cl), have been determined by a single-crystal X-ray analysis. A mononuclear trigonal-bipyramidal (for **1** and **2**), binuclear octahedral (for **3**) and binuclear trigonal-bipyramidal (for **4**) structures of the complexes were proposed mainly on the basis of spectral and magnetic properties. An $S = 3/2$–$5/2$ spin-admixed state in **1** and **2** was found to be related to the presence of $[FeCl_5]^{2-}$ ($S = 3/2$) and $[FeCl_5(H_2O)]^{2-}$ ($S = 5/2$) complex anions in **1** and **2**, as found by $^{57}$Fe Mössbauer spectroscopy. Cytotoxic activity of the complexes was determined by a calcein AM assay and $IC_{50}$ values were also estimated. For testing, human malignant melanoma cell line *G-361*, human osteogenic sarcoma cell line *HOS*, human chronic myelogenous leukaemia *K-562* and human breast adenocarcinoma cell line *MCF7* were used. The inhibition of $p34^{cdc2}$ kinase by the complexes **1** and **2**, which is known to be one of the important mechanisms responsible for cytotoxicity of cytokinin-derived compounds, was also studied. 

*Keywords:* Iron(III) and copper(II) complexes; 6-Benzylaminopurine derivatives; Cytotoxic activity; CDK inhibitor; Magnetic properties; Crystal structures

## 1. Introduction

In our previous work we have described the preparation, properties and biological activity of several copper(II) complexes with 6-(2-chlorobenzylamino)purine ($HL_2$) and 6-(3-chlorobenzylamino)purine ($HL_3$) [1]. We have showed that the composition of the prepared complexes chiefly depends on the molar reactants ratio, solvent and pH-medium used. When we have allowed to react $CuCl_2\cdot 2H_2O$ with $HL_2$ in a molar ratio of 1:2 or 2:1 in ethanol we have always obtained the octahedral binuclear copper(II) complex of the composition $[Cu_2(\mu\text{-}Cl)_2(\mu\text{-}HL_2)_2(HL_2)_2Cl_2]\cdot 2H_2O$. Likewise, the reaction of $CuCl_2\cdot 2H_2O$ with the organic ligands $HL_2$ and

* Corresponding author. Tel.: +420-68-563 4361; fax: +420-68-522 5737.
*E-mail address:* trav@risc.upol.cz (Z. Trávníček).

0020-1693/01/$ - see front matter 
PII: S0020-1693(01)00611-9

$HL_3$, in molar ratios 1:1, led in ethanol to formation of probably tetrahedral $[Cu_2(\mu\text{-}Cl)_2(HL_2)_2Cl_2]$, and $[Cu_2(\mu\text{-}Cl)_2(HL_3)_2Cl_2]$, respectively. Whereas, the complexes $[Cu_2(\mu\text{-}Cl)_2(\mu\text{-}HL_2)_2(H_2O)_2]$ and $[Cu_2(\mu\text{-}Cl)_2(\mu\text{-}HL_3)_2(H_2O)_2]$ were prepared by the reaction of $CuCl_2{\cdot}2H_2O$ with the appropriate organic ligand in ethanol in the presence of $Et_3N$, in a molar ratio 1:1:1. The above-mentioned compounds belong to a category of copper(II) complexes containing either $Cu(\mu\text{-}Cl)_2(\mu\text{-}L)_2Cu$ (L, bidentate nitrogen-donor ligand, e.g. 1,8-naphthyridine [2]) or $Cu(\mu\text{-}Cl)_2Cu$ core [3–5].

These compounds are not only studied from a basis research point of view for their interesting magnetic properties but also because of their possible both technological and biological use [6,7]. Some of the discussed complexes, actually dichloro bridged binuclear copper(II) containing the $Cu(\mu\text{-}Cl)_2Cl$ core, were also structurally classified [7].

This paper represents results in our continuing work of transition metal complexes with 6-benzylaminopurine derivatives. Ligands representing different groups of 6-benzylaminopurine derivatives having different roles in cell cycle regulation were chosen for this study. We report here the synthesis and characterization of iron(III) compounds with 2-(3-hydroxypropylamino)-6-benzylamino-9-isopropylpurine (*Bohemin*, $HL_1$) and copper(II) complexes with 6-(2-chlorobenzylamino)-purine ($HL_2$) or 6-(3-chlorobenzylamino)purine ($HL_3$) (see Scheme 1). Apart from other thinks, one of the findings of our research was discovery of a new manner in preparation of the compound $[Cu_2(\mu\text{-}Cl)_2(\mu\text{-}HL_2)_2(HL_2)_2Cl_2]$ (**3**). The other aim of the present study was to test biological activity, especially cytotoxicity of the prepared complexes and ligands used, and their ability to inhibit $p34^{cdc2}$ kinase. Special respect was given to study possible influence of complex formation on biological activity of studied compounds.

## 2. Experimental

### 2.1. Starting materials

$CuCl_2{\cdot}2H_2O$, $FeCl_3{\cdot}6H_2O$, 6-chloropurine, 2-chlorobenzylamine, 3-chlorobenzylamine and solvents used were purchased from commercial sources (Fluka co., Aldrich Co.) and used as received. Bohemin ($HL_1$) was supplied from Olchemim Co. (Olomouc, Czech Republic).

### 2.2. Preparation of $HL_2$ and $HL_3$

The compounds were prepared by slightly modified procedure as described in the literature [8] and were characterized by elemental analysis (C, H, N) and ES + mass spectra. *Anal.* Calc for $HL_2$ $C_{12}H_{10}N_5Cl_1$ (259.7): C, 55.5; H, 3.9; N, 27.0. Found: C, 55.6; H, 3.7; N, 27.1%. ES + MS: $m/z = 260$ (based on $^{35}Cl$) $[M]^+$, 224 $[M\text{–}Cl]^+$, 125 $[Cl\text{–}C_6H_4\text{–}CH_2]^+$, 91 $[C_6H_4\text{–}CH_2]^+$, 78 $[C_6H_5]^+$. *Anal.* Calc. for $HL_3$ $C_{12}H_{10}N_5Cl_1$ (259.7): C, 55.5; H, 3.9; N, 27.0. Found: C, 55.3; H, 3.9; N, 26.8%. ES + MS: $m/z = 260$ (based on $^{35}Cl$) $[M]^+$, 125 $[Cl\text{–}C_6H_4\text{–}CH_2]^+$, 90 $[C_6H_4\text{–}CH_2]^+$, 78 $[C_6H_5]^+$.

### 2.3. Preparation of the iron(III) and copper(II) complexes

#### 2.3.1. $(H^+HL_1)_2[FeCl_5]{\cdot}2H_2O$ (1)

A total of 1 mmol (340 mg) of $HL_1$ was added to a solution of $FeCl_3{\cdot}6H_2O$ (0.5 mmol, 135 mg) in 2 M HCl (20 $cm^3$). The reaction mixture was kept in ultrasonic for 5 min. Yellow solution was refluxed for 10 h and left for 5 weeks during which yellow microcrystals formed. The solid was filtered off, washed with ethanol and diethyl ether, and dried under an infra lamp at 40 °C. m.p. 113–116 °C. Yields ranged from 30 to 40%. *Anal.* Calc. for $C_{36}H_{50}N_{12}O_2Cl_5Fe_1{\cdot}(H_2O)_2$: C,

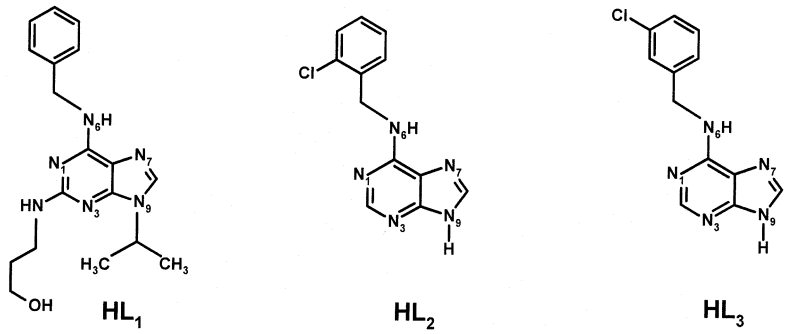


Scheme 1.

45.4; H, 5.7; N, 17.7; Cl, 18.6. Found: C, 45.3; H, 5.6; N, 17.5; Cl, 18.4%. FAB + MS ($m/z$): 341, 250, 163, 93, 75, 45. IR ($cm^{-1}$): 3200, 3060, 2740, 1840, 1684, 1602, 1532, 1508, 1446, 1408, 1376, 1278, 1242, 1200, 1172, 1060, 1040, 964, 924, 846, 756, 722, 702, 652, 604, 486.

### 2.3.2. $(H^+HL_1)_2[FeCl_5]\cdot 3H_2O$ (2)

A total of 1 mmol (340 mg) of $HL_1$ was added to a solution of $FeCl_3\cdot 6H_2O$ (1 mmol, 270 mg) in 2 M HCl (20 $cm^3$). The resulting light-yellow solution was refluxed for 4 h and left for 2 weeks during which yellow acicular microcrystals formed. Crystals were separated by filtration, washed with 2 M HCl, water, ethanol and diethyl ether, and dried under an infra lamp at 40 °C. m.p. 114–118 °C. Yields ranged from 50 to 60%. *Anal.* Calc. for $C_{36}H_{50}N_{12}O_2Cl_5Fe_1\cdot(H_2O)_3$: C, 44.6; H, 5.8; N, 17.3; Cl, 18.3. Found: C, 44.2; H, 5.9; N, 17.1; Cl, 18.5%. ES + MS ($m/z$): 681, 419, 341, 247, 157, 78. IR ($cm^{-1}$): 3220, 3050, 1686, 1632, 1604, 1542, 1510, 1444, 1392, 1376, 1276, 1230, 1210, 1170, 1060, 1040, 950, 922, 852, 756, 702, 654, 604, 486.

### 2.3.3. $[Cu_2(\mu\text{-}Cl)_2(\mu\text{-}HL_2)_2(HL_2)_2Cl_2]\cdot 2H_2O$ (3)

To a solution of $CuCl_2\cdot 2H_2O$ (1 mmol, 170 mg) in 2 M HCl (20 $cm^3$) was added the $HL_2$ ligand (1 mmol, 260 mg). The reaction mixture was kept in ultrasonic for 5 min and subsequently refluxed for 6 h. A colour of the reaction mixture changed gradually from light green to green–yellow. The precipitate which separated was filtered and washed with 2 M HCl, water, ethanol and diethyl ether, and dried under an infra lamp at 40 °C. m.p. 258 °C. Yields ranged from 60 to 80%. *Anal.* Calc. for $C_{48}H_{40}N_{20}Cl_8Cu_2\cdot(H_2O)_2$: C, 42.9; H, 3.3; N, 20.8; Cl, 21.2. Found: C, 42.7; H, 3.1; N, 20.1; Cl, 21.1%. ES + MS ($m/z$): 1305, 1051, 972, 750, 654, 617, 582, 513, 260, 78. IR ($cm^{-1}$): 3260, 3190, 3125, 3040, 2660, 1644, 1608, 1582, 1536, 1504, 1432, 1410, 1342, 1320, 1280, 1230, 1210, 1190, 1150, 1126, 1114, 1056, 1030, 970, 932, 868, 856, 756, 722, 684, 660, 610, 588, 572, 528.

### 2.3.4. $[Cu_2(\mu\text{-}Cl)_2(\mu\text{-}HL_3)_2Cl_2]$ (4)

To a solution of $CuCl_2\cdot 2H_2O$ (1 mmol, 170 mg) in 2 M HCl (20 $cm^3$) was added the organic ligand $HL_3$ (1 mmol, 260 mg). The reaction mixture was kept in ultrasonic for 5 min and light green solution was refluxed. The light green precipitate developed after 2 h and reaction mixture was refluxed for next 4 h. No change was observed and the solid was isolated by filtration, washed with 2 M HCl, water, ethanol and diethyl ether, and dried under an infra lamp at 40 ° C. m.p. 262 °C. Yields ranged from 70 to 80%. *Anal.* Calc. for $C_{24}H_{20}N_{10}Cl_6Cu_2$: C, 36.6; H, 2.6; N, 17.8; Cl, 27.0. Found: C, 36.8; H, 2.6; N, 17.3; Cl, 27.1%. ES + MS ($m/z$): 1051, 972, 750, 654, 617, 582, 513, 260, 78. IR ($cm^{-1}$): 3292, 3224, 3140, 2800–2600, 1632, 1600, 1578, 1536, 1508, 1426, 1404, 1346, 1312, 1270, 1230, 1206, 1186, 1144, 1114, 1076, 1030, 976, 928, 892, 868, 856, 796, 784, 698, 684, 676, 600, 572, 552, 444.

### 2.4. Elemental analyses

Elemental analyses (C, H, N) were performed on an EA1108 CHN analyser (Fisons Instruments). The chlorine content was determined by the Schöniger method.

### 2.5. Spectroscopic studies

Electronic absorption spectra (diffuse-reflectance) were recorded on a SPECORD M40 (Carl Zeiss Jena) within the 40 000–1100 $cm^{-1}$ range. IR spectra were recorded on a SPECORD IR 80 instrument (Carl Zeiss Jena) in Nujol mulls (4000–400 $cm^{-1}$).

ES + mass spectra were recorded for **1**, **3** and **4** using direct probe on a Waters ZMD 2000 mass spectrometer. The mass-monitoring interval was 10–1500 amu. The spectra were collected using 3.0 second cyclical scans and applying sample cone voltage 20, 30 or 40 V at source block temperature 80 °C, desolvation temperature 150 °C and desolvation gas flow rate 200 l $h^{-1}$. Mass spectrometer was directly coupled to a MassLynx data system. FAB + mass spectra for **2** were obtained using direct probe on double-focusing magnetic sector mass spectrometer (JMS-SX 102, JEOL). The ion source temperature was 55 °C. Desorption was generated with a beam of 3 kV xenon atoms at an emission current of 10 mA. Full scan analyses were performed for a mass range 10–1400 $m/z$. Data were processed by a JEOL MD-7010 data system. All interpretations of $m/z$ are based on $^{35}Cl$ and $^{63}Cu$.

The transmission Mössbauer spectra were collected at 300 and 30 K using a Mössbauer spectrometer in constant acceleration mode with a $^{57}Co(Rh)$ source. A cryostat with closed He-cycle (Janis Research Company, USA) was used as a refrigerating system that allowed to work in a temperature range of 12–300 K.

### 2.6. Magnetic data

The susceptibility studies were performed on powdered samples with the average weight 60 mg using a Quantum Design MPM-5S SQUID magnetometer. All measurements were conducted in a field of 0.9 T. Measurements were made in the range 35.0–300 K for **3** and 4.5–300 K for all remaining compounds. The molar susceptibilities were corrected for diamagnetism using Pascal's constants [9]. Conductivity measurements were made with an OK 102 $l^{-1}$ conductometer (Radelkis, Budapest) in DMFA at 25 °C. The concentration of the complexes in solutions was $10^{-3}$ mol $dm^{-3}$ [10].

Table 1
Crystal data and structure refinement for $HL_2{\cdot}2H_2O$ and $H^+HL_3$–Cl

| | $HL_2{\cdot}2H_2O$ | $H^+HL_3$–Cl |
|---|---|---|
| Empirical formula | $C_{12}H_{14}ClN_5O_2$ | $C_{12}H_{11}Cl_2N_5$ |
| Formula weight | 295.73 | 296.16 |
| Temperature (K) | 120(2) | 293(2) |
| Wavelength (Å) | 0.71073 | 0.71073 |
| Crystal system | triclinic | monoclinic |
| Space group | $P\bar{1}$ | $P2_1/c$ |
| Unit cell dimensions | | |
| $a$ (Å) | 6.9289(7) | 18.791(2) |
| $b$ (Å) | 8.8180(11) | 8.8630(8) |
| $c$ (Å) | 11.5462(12) | 8.1371(9) |
| $\alpha$ (°) | 69.751(10) | 90 |
| $\beta$ (°) | 84.838(8) | 96.513(9) |
| $\gamma$ (°) | 80.017(9) | 90 |
| $V$ (Å) | 651.50(12) | 1346.4(2) |
| $Z$ | 2 | 4 |
| $D_{calc}$ (g cm$^{-3}$) | 1.508 | 1.461 |
| $\mu$ (mm$^{-1}$) | 0.303 | 0.475 |
| $F(000)$ | 308 | 608 |
| Crystal size (mm) | $0.50\times0.30\times0.20$ | $0.50\times0.40\times0.15$ |
| $\theta$ Range (°) | 3.59–25.00 | 3.41–24.99 |
| Index ranges | $-8\le h\le7$ | $-22\le h\le22$ |
| | $-10\le k\le10$ | $-10\le k\le10$ |
| | $-13\le l\le13$ | $-9\le l\le6$ |
| Reflections collected | 3558 | 7917 |
| Independent reflections | 2220 | 2354 |
| | [$R_{int}=0.0342$] | [$R_{int}=0.0323$] |
| Max./min. transmission | 0.9418 and | 0.9322 and |
| | 0.8632 | 0.7971 |
| Refinement method | full-matrix least-squares on $F^2$ | |
| Data/restraints/parameters | 2220/0/229 | 2354/0/216 |
| Goodness-of-fit on $F^2$ | 0.983 | 0.992 |
| Final $R$ indices [$I>2\sigma(I)$] | | |
| $R_1$ | 0.0324 | 0.0451 |
| $wR_2$ | 0.0854 | 0.1293 |
| $R$ indices (all data) | | |
| $R_1$ | 0.0363 | 0.0521 |
| $wR_2$ | 0.0879 | 0.1347 |
| Extinction coefficient | 0.004(3) | none |

### 2.7. X-ray data collection and structure refinement for 6-(2-chlorobenzylamino)purine dihydrate solvate, $HL_2{\cdot}2H_2O$, and 6-(3-chlorobenzylamino)purinium chloride, $H^+HL_3$–Cl

X-ray data were collected at 120 K (for $HL_2{\cdot}2H_2O$) and 293 K (for $H^+HL_3$–Cl) on a four-circle $\kappa$-axis KUMA KM-4 diffractometer equipped with an Oxford Cryostream cooler using graphite-monochromated Mo Kα radiation. Data collections for the organic ligands were performed using a CCD detector (KUMA Diffraction, Wroclaw). KUMA KM4RED software was used for data reduction. The structures were solved using the direct methods [SHELXS-97] [11] and refined on $F^2$ using full-matrix least-squares procedure [SHELXL-97] [12] with weight: $w=1/[\sigma^2(F_o^2)+(0.0481P)^2+0.4289P]$ for $HL_2{\cdot}2H_2O$, and $w=1/[\sigma^2(F_o^2)+(0.0890P)^2+0.5986P]$ for $H^+HL_3$–Cl, respectively, where $P=(F_o^2+2F_c^2)/3$. All hydrogens in both structures were located in difference Fourier maps and all their parameters were refined. The largest peak and hole on the final difference map were 0.36 [0.89 Å from O(1)] and −0.30 [0.91 Å from C(10)] e Å$^{-3}$ for $HL_2{\cdot}2H_2O$, and 0.36 [1.02 Å from Cl(1)] and −0.59 [0.82 Å from Cl(1)] e Å$^{-3}$ for $H^+HL_3$–Cl, respectively. Full crystallographic data may be found in Table 1. Selected bond distances and angles are given in Table 2.

### 2.8. Biological activity testing

Human malignant melanoma cell line *G-361*, human osteogenic sarcoma cell line *HOS*, human chronic myelogenous leukaemia cell line *K-562* and human breast adenocarcinoma cell line *MCF7* were used for a cytotoxicity determination of the prepared complexes by calcein AM assay, as it was described previously in more details [1,13]. Briefly, the tumour cells were maintained in plastic tissue culture flasks and grown on Dulbecco's modified Eagle's cell culture medium (DMEM) at 37 °C in 5% $CO_2$ atmosphere and 100% humidity. The cell suspension of approximate density $1.25\times10^5$ cells ml$^{-1}$ was redistributed into 96-well microtitre plates (Nunc, Denmark). After 12 h of preincubation, the tested compounds (in the 0.5–200 μM range) were added. Incubation lasted for 72 h. At the end of this period, the cells were incubated for 1 h with calcein AM and fluorescence of the live cells was measured at 485/538 nm (ex/em) with a Fluoroskan Ascent (Labsystems, Finland). $IC_{50}$ values, the drug concentrations lethal to 50% of the tumour cells, were estimated.

Kinase p34$^{cdc2}$/cyclin B was produced in Sf9 insect cells co-infected with baculoviral constructs [12]. Kinase activity was assayed with 1 mg ml$^{-1}$ histone H1 in the presence of 15 μM [$\gamma$-$^{32}$P] ATP (500–1000 cpm pmol$^{-1}$) in final volume of 10 μl. After 15 min the reactions were stopped by addition of 3 × SDS sample buffer and separated electrophoretically on SDS polyacrylamide gel [1,12]. Final measurement of phosphorylated proteins was done using a digital imaging system.

The stability of tested complexes in the media used was monitored by measurement of UV–Vis spectra. No significant changes in the maxima of the absorption peaks were observed after 24 h.

## 3. Results and discussion

The reaction between $FeCl_3{\cdot}6H_2O$ and $HL_1$ in 2M HCl in a molar ratio 1:1 or in a molar ratio 1:2 yielded mononuclear complexes $(H^+HL_1)_2[FeCl_5]{\cdot}xH_2O$ ($x=2$ for **1** and $x=3$ for **2**), while the reaction of $CuCl_2{\cdot}2H_2O$ with $HL_2$ or $HL_3$ (in a molar ratio 1:1) in 2M HCl led to formation of binuclear complexes $[Cu_2(\mu\text{-}Cl)_2(\mu\text{-}HL_2)_2(HL_2)_2(Cl)_2]{\cdot}2H_2O$ (**3**) and $[Cu_2(\mu$-

Table 2
Selected bond lengths (Å) and angles (°) for $HL_2 \cdot 2H_2O$ and $H^+ HL_3$–Cl

| $HL_2 \cdot 2H_2O$ | | $H^+HL_3$–Cl | |
|---|---|---|---|
| *Bond lengths* | | | |
| Cl(1)–C(12) | 1.7441(17) | Cl(1)–C(13) | 1.745(3) |
| N(1)–C(6) | 1.350(2) | N(1)–C(6) | 1.361(3) |
| N(1)–C(2) | 1.347(2) | N(1)–C(2) | 1.306(3) |
| N(3)–C(2) | 1.333(2) | N(3)–C(2) | 1.328(3) |
| N(3)–C(4) | 1.351(2) | N(3)–C(4) | 1.356(3) |
| N(6)–C(6) | 1.343(2) | N(6)–C(6) | 1.323(3) |
| N(6)–C(10) | 1.453(2) | N(6)–C(10) | 1.452(3) |
| N(7)–C(8) | 1.318(2) | N(7)–C(8) | 1.339(3) |
| N(7)–C(5) | 1.381(2) | N(7)–C(5) | 1.362(3) |
| N(9)–C(8) | 1.365(2) | N(9)–C(8) | 1.322(3) |
| N(9)–C(4) | 1.374(2) | N(9)–C(4) | 1.356(3) |
| C(6)–C(5) | 1.415(2) | C(6)–C(5) | 1.410(3) |
| C(4)–C(5) | 1.380(2) | C(4)–C(5) | 1.373(3) |
| C(10)–C(11) | 1.515(2) | C(10)–C(11) | 1.508(4) |
| C(11)–C(16) | 1.388(2) | C(11)–C(16) | 1.371(4) |
| C(11)–C(12) | 1.397(2) | C(11)–C(12) | 1.383(4) |
| C(12)–C(13) | 1.385(3) | C(12)–C(13) | 1.370(4) |
| C(13)–C(14) | 1.387(3) | C(13)–C(14) | 1.358(5) |
| C(14)–C(15) | 1.386(3) | C(14)–C(15) | 1.354(6) |
| C(15)–C(16) | 1.391(3) | C(15)–C(16) | 1.395(6) |
| *Bond angles* | | | |
| C(6)–N(1)–C(2) | 118.81(14) | C(6)–N(1)–C(2) | 119.10(19) |
| C(2)–N(3)–C(4) | 111.32(14) | C(2)–N(3)–C(4) | 117.6(2) |
| C(6)–N(6)–C(10) | 123.97(15) | C(6)–N(6)–C(10) | 123.0(2) |
| C(8)–N(7)–C(5) | 103.68(15) | C(8)–N(7)–C(5) | 106.8(2) |
| C(8)–N(9)–C(4) | 106.19(14) | C(8)–N(9)–C(4) | 102.60(18) |
| N(6)–C(6)–N(1) | 120.33(15) | N(6)–C(6)–N(1) | 118.7(2) |
| N(6)–C(6)–C(5) | 121.74(16) | N(6)–C(6)–C(5) | 123.7(2) |
| N(1)–C(6)–C(5) | 117.93(15) | N(1)–C(6)–C(5) | 117.55(19) |
| N(3)–C(2)–N(1) | 128.48(17) | N(3)–C(2)–N(1) | 126.0(2) |
| N(3)–C(4)–N(9) | 127.90(15) | N(3)–C(4)–N(9) | 127.91(19) |
| N(3)–C(4)–C(5) | 126.65(15) | N(3)–C(4)–C(5) | 119.7(2) |
| N(9)–C(4)–C(5) | 105.45(15) | N(9)–C(4)–C(5) | 112.40(19) |
| C(4)–C(5)–N(7) | 111.14(14) | C(4)–C(5)–N(7) | 104.41(19) |
| C(4)–C(5)–C(6) | 116.81(15) | C(4)–C(5)–C(6) | 120.06(19) |
| N(7)–C(5)–C(6) | 132.06(16) | N(7)–C(5)–C(6) | 135.53(19) |
| N(7)–C(8)–N(9) | 113.54(16) | N(7)–C(8)–N(9) | 113.8(2) |
| N(6)–C(10)–C(11) | 114.74(14) | N(6)–C(10)–C(11) | 112.28(19) |
| C(16)–C(11)–C(12) | 116.96(16) | C(16)–C(11)–C(12) | 118.6(3) |
| C(16)–C(11)–C(10) | 123.37(15) | C(16)–C(11)–C(10) | 120.9(3) |
| C(12)–C(11)–C(10) | 119.67(15) | C(12)–C(11)–C(10) | 120.5(2) |
| C(13)–C(12)–C(11) | 122.56(16) | C(13)–C(12)–C(11) | 120.2(3) |
| C(13)–C(12)–Cl(1) | 118.29(13) | C(12)–C(13)–Cl(1) | 118.7(2) |
| C(11)–C(12)–Cl(1) | 119.15(13) | C(14)–C(13)–Cl(1) | 119.6(3) |
| C(14)–C(13)–C(12) | 119.08(16) | C(14)–C(13)–C(12) | 121.7(3) |
| C(13)–C(14)–C(15) | 119.80(17) | C(13)–C(14)–C(15) | 118.5(3) |
| C(14)–C(15)–C(16) | 120.09(17) | C(14)–C(15)–C(16) | 121.4(3) |
| C(11)–C(16)–C(15) | 121.50(16) | C(11)–C(16)–C(15) | 119.6(4) |

$Cl)_2(\mu\text{-}HL_3)_2(Cl)_2]$ (**4**) {$HL_2$ = 6-(2-chlorobenzylamino)purine, $HL_3$ = 6-(3-chlorobenzylamino)purine}. Their electronic spectral, magnetic and conductivity data are listed in Table 3. The diffuse-reflectance electronic spectra of complexes **1** and **2** exhibit band at 26 800 and 27 000 $cm^{-1}$, respectively, which can be assigned to d–d transitions. The maxima at 32 000 $cm^{-1}$ for **1** and 32 100 $cm^{-1}$ for **2** are due to CT transitions. In the case of **3** and **4**, the maxima observed at 12 600 and 12 400 $cm^{-1}$, respectively, may be connected with the d–d transitions, while the shoulders near 28 000 $cm^{-1}$ are attributable to the $\pi \rightarrow$ copper(II) LMCT transitions. The maxima ranging from 28 400 to 35 000 $cm^{-1}$ are probably due to internal ligand or ligand-to-metal charge-transfer transitions [14,15].

In IR spectra of all complexes, the bands observed between 1630 and 1644 $cm^{-1}$ may be assigned to the $\nu$(C=N) stretch vibration of the heterocyclic ring. The bands at approximately 1604, 1510 and 1420–1440 $cm^{-1}$ are assignable to the $\nu$(C=C) vibration, while the maxima appearing in the region 910–660 $cm^{-1}$ are due to skeletal vibrations of aromatic rings and thus confirm the presence of the $HL_1$, $HL_2$ or $HL_3$ ligands in the compounds **1**–**4**. The presence of chlorine attached directly to the aromatic ring is apparent from the band at 1114–1150 $cm^{-1}$ found in the IR spectra of compounds **3** and **4**. The bands appearing in spectra of all complexes near 3050 and 3240 $cm^{-1}$ can be connected with $\nu$(C–H) and $\nu$(N–H) vibrations, respectively [16,17].

The molar conductance values for the complexes **1** and **2** as formulated in Table 1 show on considerable dissociation of the compounds in DMFA solution indicating thus that they behave as electrolytes of the 2:1 type [10]. The values of $\lambda_M$ found for **3** and **4** clearly indicate a non-ionic feature of the complexes in the solvent used.

### 3.1. Magnetic and $^{57}$Fe Mössbauer data

The magnetic properties of complexes **1** and **2** have been studied in the temperature range from 4.5 to 300 K. The temperature variations of magnetic susceptibility and magnetic moment for **1** are shown in Fig. 1. The effective magnetic moment was calculated as $\mu_{eff} = 2.828(\chi_M T)^{1/2} \mu_B$. It can be seen from the figure, that the effective magnetic moment is nearly constant in the temperature interval 15–300 K with the values of 4.21–4.23 $\mu_{eff}/\mu_B$ for **1**, and 4.51–4.48 $\mu_{eff}/\mu_B$ for **2**, respectively. Below 15 K, a slight decrease can be related to the presence of a weak antiferromagnetic interaction for both cases. The values of $C$ and $\theta$ were determined using Curie–Weiss law, $\chi_M = C/(T-\theta)$, and are equal to 2.343(3) $cm^3$ K $mol^{-1}$ and $-0.87(1)$ K for **1**, and 2.691(5) $cm^3$ K $mol^{-1}$ and 0.90(1) K for **2**, respectively. At room temperature $\chi_M T$ value is equal to 2.24 $cm^3$ K $mol^{-1}$ (for **1**) and 2.51 $cm^3$ K $mol^{-1}$ (for **2**), which is significantly higher than anticipated for a pure $S = 3/2$ state ($\approx 1.876$ $cm^3$ K $mol^{-1}$), but considerable lower than anticipated for a pure $S = 5/2$ state ($\approx 4.377$ $cm^3$ K $mol^{-1}$). On cooling, $\chi_M T$ value is nearly constant down to 15 K, and then smoothly decreases. At 4.5 K,

Table 3
Colours, magnetic, electronic spectral and molar conductivity data for the complexes

| Compound | Colour | $\mu_{eff}/\mu_B$ | $J$ ($cm^{-1}$) | $g$ | Absorption maxima [b] $\times 10^3$ ($cm^{-1}$) | $\lambda_M$ [c] (S $cm^2$ $mol^{-1}$) |
|---|---|---|---|---|---|---|
| **1** | Yellow | 4.23 (300 K)–3.95 (4.5K) | | | 26.8, 32.0 | 122 |
| **2** | Yellow | 4.48 (300 K)–4.22 (4.5 K) | | | 27.0, 32.1 | 126 |
| **3** | Green–yellow | 1.61 (295 K)–0.49 (35 K) [a] | −61.6(6) | 2.00 | 12.6, 23.0, 29.0, 34.0 | 24 |
| **4** | Light–green | 1.93 (300 K)–0.13 (4.5 K) [a] | −40.89(7) | 1.982(4) | 12.4, 22.8, 28.4, 35.0 | 14 |

[a] Value per one Cu(II) ion.
[b] Diffuse-reflectance spectra measured by Nujol technique.
[c] Measured in DMFA.

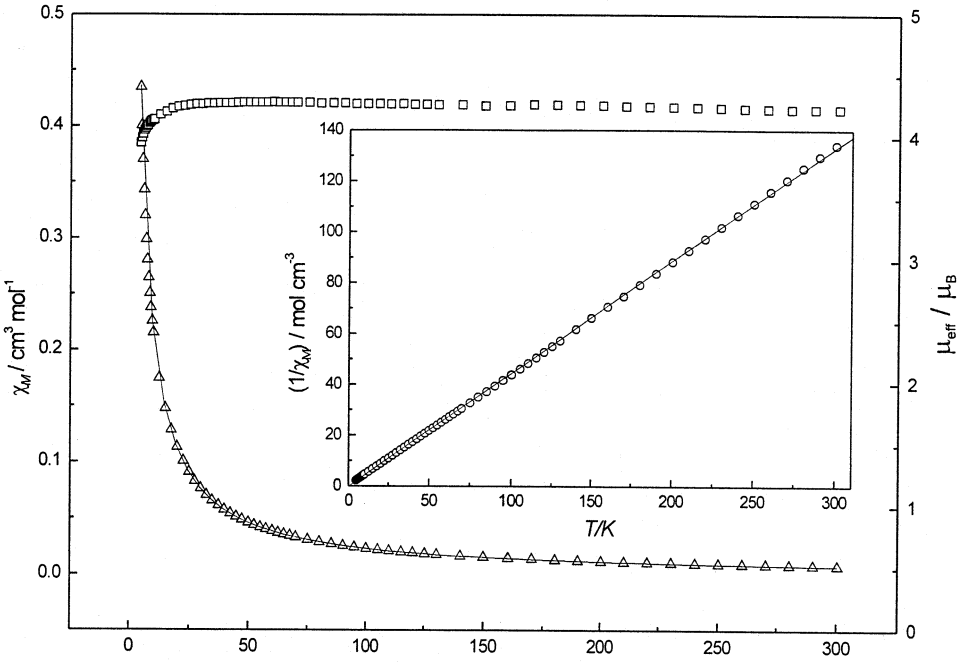


Fig. 1. Thermal dependence of $\chi_M$ ($\rho$) and $\mu_{eff}/\mu_B$ ($\leq$) for **1**. The solid line represents the best-fit to the Curie–Weiss law. The insert shows the thermal dependence of $1/\chi_M$.

$\chi_M T$ is equal to 1.95 $cm^3$ K $mol^{-1}$ (for **1**), and 2.23 $cm^3$ K $mol^{-1}$ (for **2**), respectively. From the above mentioned magnetochemical data for **1** and **2** we may conclude that both complexes belong to the group of spin-admixed iron(III) compounds with $S = 3/2$–$5/2$ [18]. Thus, we suppose that the coordination geometry in $[FeCl_5]^{2-}$ is dominantly trigonal-bipyramidal (within the $S = 3/2$ state) encountered with six-coordinate octahedral $[FeCl_5(H_2O)]^{2-}$ with an $S = 5/2$ ground state. This conclusion may be supported by $^{57}$Fe Mössbauer spectroscopy. Taking into account the low content of iron in compounds **1** and **2**, the spectra were recorded not only at room temperature but also at 30 K to improve the recoil-less fraction. The spectra measured at 30 K are depicted in Fig. 2, while the hyperfine parameters are given in Table 4. Both spectra consist of three subspectra, i.e. $Fe^{3+}$ doublet, $Fe^{3+}$ singlet and $Fe^{2+}$ doublet. The parameters [$\delta = 0.30$, $\Delta = 0.45$ mm $s^{-1}$ for **1**, $\delta = 0.31$, $\Delta = 0.45$ mm $s^{-1}$ for **2**] of the $Fe^{3+}$ doublet clearly characterize the presence of the $[FeCl_5]^{2-}$ complex anion with $D_{3h}$ symmetry in both compounds. The data are also consistent with the results obtained on similar systems containing trigonal-bipyramidal $[FeCl_5]^{2-}$ anion, such as **I**[Fe(III)$Cl_5$] ($\delta = 0.21$, $\Delta = 0.42$ mm $s^{-1}$; **I** = tetramethylpiperazinium) [19], **II**[Fe(III)$Cl_5$] ($\delta = 0.312$, $\Delta = 0.50$ mm $s^{-1}$; **II** = tetramethylimidazolium) [19] and **II-I**[Fe(III)$Cl_5$] ($\delta = 0.27$, $\Delta = 0.34$ mm $s^{-1}$; **III** = diquaternized cation obtained from diazabicyclo[2.2.2]-octane, DABCO) [20]. The $Fe^{3+}$ singlet with $\delta = 0.21$ mm $s^{-1}$ may be probably connected with the presence of octahedrally coordinated iron(III) in $[FeCl_5(H_2O)]^{2-}$. A molar ratio of $[FeCl_5]^{2-}$: $[FeCl_5(H_2O)]^{2-}$ calculated from areas of component subspectra was found to be

51.5: 29.7% in **1**, and 50.0: 39.1% in **2**, respectively. The percentages of subspectra areas indicate that $[FeCl_5]^{2-}$ with trigonal-bipyramidal arrangement dominates in both complexes. This conclusion is in good agreement with magnetic data. A doublet with parameters corresponding to $Fe^{2+}$ observed in both Mössbauer spectra is probably connected with admixture of iron(II) phase in the starting material $FeCl_3 \cdot 6H_2O$.

The room temperature magnetic moment of **3** per Cu is equal to 1.61 $\mu_{eff}/\mu_B$ at 295 K and gradually decrease with decreasing temperature down to 34 K, where the $\mu_{eff} = 0.49\ \mu_B$ (see Fig. 3), suggesting on the presence of an antiferromagnetic interaction between the copper(II) ions. Against to this, the $\chi_M$ values per dimer increase up to a maximum at approximately 110 K (the Neel's temperature) and consequently decrease up to 35 K. The experimentally observed molar magnetic susceptibility data (per dimer) were treated using the (Eq. (1)), which includes a corrective term, $\rho$, for non-coupled copper(II) impurity and the temperature-independent paramagnetism, $N\alpha$.

$$\chi_M = \frac{2N\beta^2 g^2}{3kT} \frac{1-\rho}{[1+1/3\exp(-2J/kT)]} + \frac{N\beta^2 g^2 \rho}{2kT} + 2N\alpha. \quad (1)$$

Keeping $g$ fixed at 2.0 and $N\alpha$ at $60 \times 10^{-6}$ cm$^3$ mol$^{-1}$, the $J$, and $\rho$ parameters were determined by non-linear regression analysis. The best-fit parameters are: $J = -61.6(6)$ cm$^{-1}$ and $\rho = 0.017(3)$.

Variable temperature magnetic susceptibility measurements over the temperature range 4.5–300 K were used to study of magnetic properties of complex **4**. A plot of the molar magnetic susceptibilities ($\chi_M$) and the effective magnetic moment ($\mu_{eff}/\mu_B$) versus temperature is shown in Fig. 4. The $\mu_{eff}$ value of **4** at room temperature is 1.93 $\mu_B$ per Cu. As the temperature is decreased, the magnetic moment for **1** is slowly reduced to 1.48 $\mu_B$ at approximately 100 K, and then sharply decreases to a minimum value of 0.13 $\mu_B$ at 4.5 K. As can be seen from the Fig. 4, a maximum in the magnetic susceptibility is observed at 70 K (the Neel's point) indicating thus a medium strength antifferomagnetic interaction between the paramagnetic Cu(II) cen-

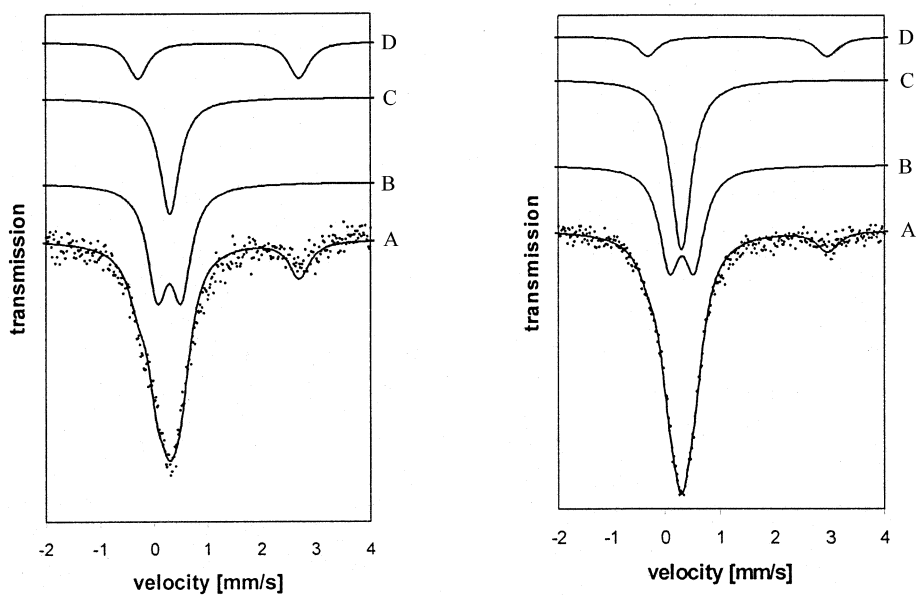


Fig. 2. The Mössbauer spectra for **1** (left) and **2** (right) at measured 30 K. **A** – the best-fit of experimental data, **B** – $Fe^{3+}$ doublet in $[FeCl_5]^{2-}$, **C** – $Fe^{3+}$ singlet in $[FeCl_5(H_2O)]^{2-}$, **D** – $Fe^{2+}$ doublet.

Table 4
Mössbauer parameters for **1** and **2**

| Compound | Doublet of $[FeCl_5]^{2-}$ | | | Singlet of $[FeCl_5(H_2O)]^{2-}$ | | | Doublet of $Fe^{2+}$ | | |
|---|---|---|---|---|---|---|---|---|---|
| | $\delta$ (mm s$^{-1}$) | $\Delta$ (mm s$^{-1}$) | $A$ (%) | $\delta$ (mm s$^{-1}$) | $\Delta$ (mm s$^{-1}$) | $A$ (%) | $\delta$ (mm s$^{-1}$) | $\Delta$ (mm s$^{-1}$) | $A$ (%) |
| **1** | 0.30 | 0.45 | 51.5 | 0.31 | 0 | 29.7 | 1.21 | 3.00 | 18.8 |
| **2** | 0.31 | 0.45 | 50.0 | 0.31 | 0 | 39.1 | 1.33 | 3.27 | 10.9 |

$\delta$, isomer shift related to iron; $\Delta$, quadrupole splitting; $A$, percentage of subspectrum area related to iron content.

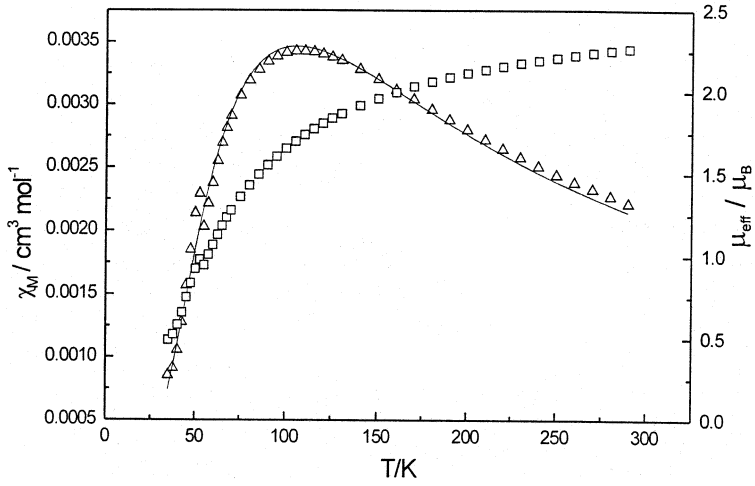


Fig. 3. Thermal dependence of $\chi_M$ ($\rho$) and $\mu_{eff}/\mu_B$ ($\leq$) for **3**. The solid line represents the best-fit to the Eq. (1) (see text). Values of $\chi_M$ and $\mu_{eff}/\mu_B$ are given per molecule.

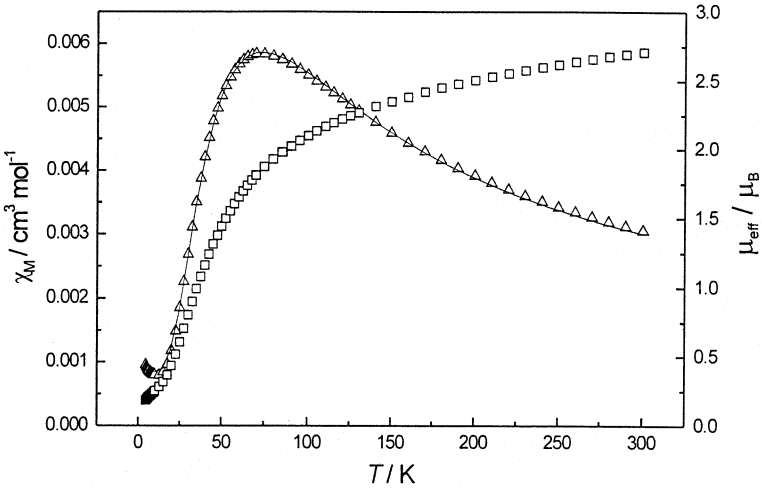


Fig. 4. Thermal dependence of $\chi_M$ ($\rho$) and $\mu_{eff}/\mu_B$ ($\leq$) for **4**. The solid line represents the best-fit to the Eq. (1) (see text). Values of $\chi_M$ and $\mu_{eff}/\mu_B$ are given per molecule.

tres. Below this temperature, the $\chi_M$ value decreases to a minimum value at 12.5 K. Consequential increasing in the magnetic susceptibility below 12.5 K is attributable to a small amount of monomeric impurity. The observed magnetic susceptibility data for dimer were fitted to the (Eq. (1)). The best-fit parameters of $g, J, \rho$ and $N\alpha$ using (Eq. (1)) were obtained by a non-linear fitting procedure with the Marquardt optimization algorithm. The following parameters were obtained: $g = 1.982(4)$, $J = -40.89(7)$ $cm^{-1}$, $\rho = 0.0003(1)$, and $N\alpha = 4.1(1) \times 10^{-5}$ $cm^3$ $mol^{-1}$.

### 3.2. Mass spectroscopy

ES+ mass spectra were measured for the complexes **2**, **3** and **4**. The ES+ mass spectrum of **2**, likewise the FAB+ mass spectrum of **1**, revealed a molecular peak at 341 $m/z$ clearly identifying the $HL_1$ molecule. The presence of the organic part of the molecules ($HL_2$ or $HL_3$) in the complexes **3** and **4** is evident from the dominant peaks at 260 $m/z$, representing the molecular peaks of $HL_2$ and $HL_3$. Consecutively, the peaks at 125, 91 and 78 $m/z$ were also observed and they may be connected with the fragments $[Cl–C_6H_5–CH_2]^+$, $[C_6H_5–CH_2]^+$, and $[C_6H_5]^+$, respectively. The peaks observed in ES+ mass spectra of **3** and **4** at 654, 617, 582, 512 $m/z$ may be related to fragments of the mononuclear species $[Cu_1(HL)_2Cl_2]^+$, $[Cu_1(HL)_2Cl_1]^+$, $[Cu_1(HL)_2]^+$, and $[Cu_1(HL–Cl)_2]^+$ (where HL=$HL_2$ or $HL_3$). Whilst, the peak at 752 $m/z$ belongs probably to a dicopper(II) fragment $[Cu_2Cl_2(HL)(HL–Cl)]^+$. The observation of peaks at 750 and 387 $m/z$, assignable to dicopper(II) fragments $[Cu_2(HL)_2Cl_3]^+$ or $[Cu_2Cl_2(HL)(HL–Cl)]^+$, and $[Cu_2(HL)_1]^+$, respectively, is typical for binuclear complexes **3** and **4**. The presence of the fragment

$[Cu_2Cl_4(HL)_4]^+$ in the ES+ spectrum of **3** is evident from the peak at 1304 $m/z$.

We can conclude, on the basis of results following from physical measurements, that the complexes **1** and **2** are mononuclear consisting of the trigonal-bipyramidal complex anion $[FeCl_5]^{2-}$ and two protonized organic molecules $H^+HL_1$ situated outside of the coordination sphere of the Fe(III) ions. Whereas, the complexes **3** and **4** have the binuclear structures as shown in Figs. 5 and 6, respectively. We suppose that both copper(II) atoms in complex **3** are six-coordinated and bridged by two chloride ions and two $HL_2$ ligands which connect two central atoms through N(3) and N(9) atoms of $HL_2$. The remaining two $HL_2$ and two chloride anions are bonded as terminal. In contrast, both copper(II) ions in complex **4** are five-coordinated probably in trigonal-bipyramidal arrangement. Thus, the central atoms in **4** are bridged by two chlorides and by two $HL_3$ molecules, whereas two remaining chlorides are again bonded as terminal. This assumption both coordination geometry around the Cu-atoms and bridging mode in complexes **3** and **4** may be supported by the values of exchange integral, $J = -61.6(6)$ and $-40.89(7)$ $cm^{-1}$, as found for **3** and **4**, respectively. This value is higher than was observed in dichloro-bridged dicopper(II) systems containing the $Cu(\mu\text{-}Cl)_2Cu$ core which are the most frequently either slightly antiferromagnetic {$J = -8$ $cm^{-1}$ in $[Cu_2(\mu\text{-}Cl)_2(TMSO)_4Cl_2]$, where TMSO = tetramethylene sulfoxide [4]; $J = -3.7$ $cm^{-1}$ in $[Cu(2\text{-pic})_2Cl_2]_2$, where 2-pic = 2-methylpyridine [21]} or ferromagnetic {$J = +3.15$ and $+0.31$ $cm^{-1}$ in $[Cu(dmgH)Cl_2]_2$, where dmgH = dimethylglyoxime, as referred in [22,23], respectively; $J = +40$ $cm^{-1}$ in $(Ph_4As)_2[Cu_2Cl_6]$ [24]} as described and compared in the literature [7]. Thus, we suppose that the complex **4** has the same structure as determined by a single crystal X-ray analysis for $[Cu_2(\mu\text{-}Cl)_2(\mu\text{-}ntphd_2)_2Cl_2]$ (where ntphd = 1,8-naphthyridine) [2], even if the last-mentioned structure shows a strong antiferromagnetic coupling with $J = -139$ $cm^{-1}$ [25].

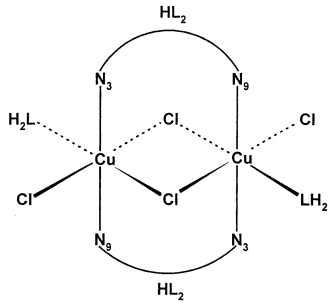


Fig. 5. Tentative structure for **3**.

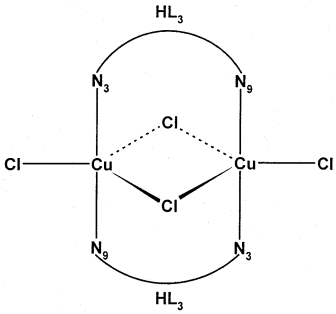


Fig. 6. Tentative structure for **4**.

### 3.3. Structural description of 6-(2-chlorobenzylamino)purine dihydrate solvate, $HL_2{\cdot}2H_2O$, and 6-(3-chlorobenzylamino)purinium chloride, $H^+HL_3$–Cl

The structure of $HL_2{\cdot}2H_2O$ in its electroneutral form is depicted in Fig. 7, while a drawing of a protonized form of $HL_3$, $H^+HL_3$–Cl, is shown in Fig. 8. As can be seen from Table 2, selected bond lengths and angles in both structures are quite similar. However, significant differences in some bond angles of the purine rings (Table 2) are due to proton shifts on the atoms N(3), N(7) and N(9). In an electroneutral form of $HL_2{\cdot}2H_2O$, the hydrogen atoms are bonded to C(2) and N(9) atoms of a purine ring. Moreover, the $H^+HL_3$–Cl molecule is also protonized on the N(3) atom in acidic medium and the hydrogen atom bonded to N(9) in the former structure is moved to N(7) in the this structure. There are no significant deviations from planarity both in purine (plane 1) and phenyl (plane 2) rings in both structures [26]. The dihedral angle between the plane 1 and plane 2 is equal to 79.5(2)° in $HL_2{\cdot}2H_2O$ and 82(1)° in $H^+HL_3$–Cl.

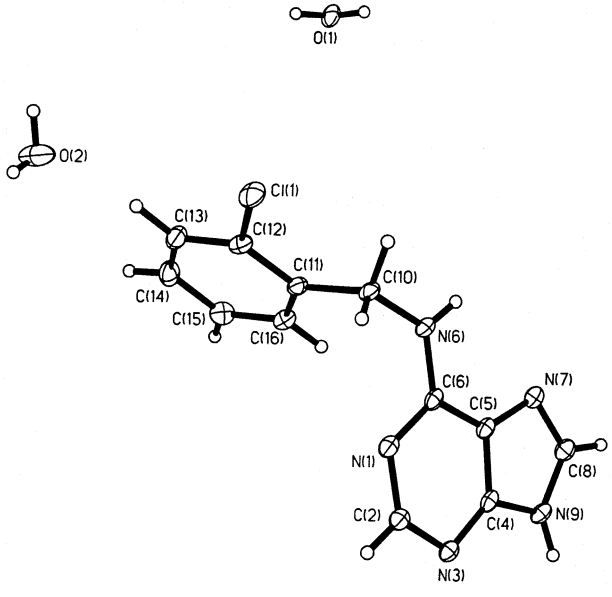


Fig. 7. Molecular structure of 6-(2-chlorobenzylamino)purine dihydrate solvate (**$HL_2{\cdot}2H_2O$**). Thermal ellipsoids are plotted at the 50% probability level.

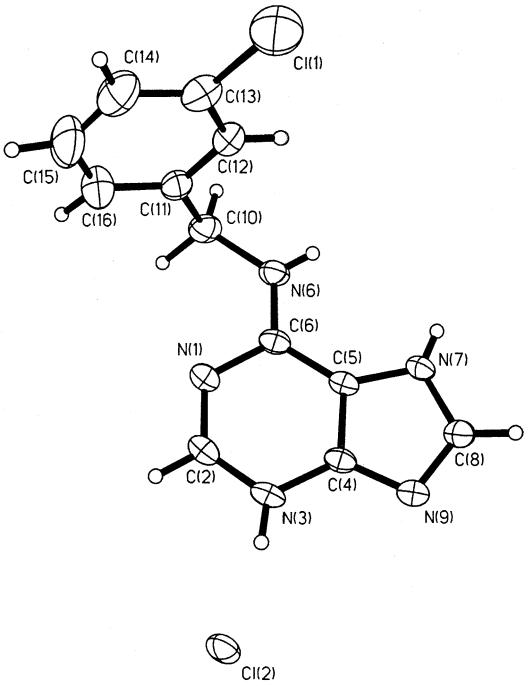


Fig. 8. Molecular structure of 6-(3-chlorobenzylamino)purinium chloride, (**$H^+HL_3$–Cl**). Thermal ellipsoids are plotted at the 30% probability level.

Table 5
$IC_{50}$ (μM) assessed by calcein AM assay of surviving tumour cells

| Compound | Cell line | | | |
|---|---|---|---|---|
| | *G-361* | *HOS* | *K-562* | *MCF7* |
| **1** | 23 | 31 | 29 | 24 |
| **2** | 22 | 27 | 26 | 21 |
| **3** | 17 | 18 | 31 | 24 |
| **4** | 36 | 38 | 32 | 39 |
| $H^+HL_1$–Cl | 55 | 60 | 96 | 58 |
| $HL_2$ | 95 | >167 | 96 | 129 |
| $HL_3$ | >167 | >167 | >167 | >167 |
| $FeCl_3·6H_2O$ | >200 | >200 | >200 | >200 |
| $CuCl_2·2H_2O$ | 100 | >100 | >100 | >100 |

The tumor cell lines (*G-361*, human malignant melanoma; *HOS*, human osteogenic sarcoma; *K-562*, human chronic myelogenous leukaemia; *MCF7*, human breast adenocarcinoma) were treated with solution of the tested compound in the 0.5–200 μM range for 72 h at 37 °C, 5% $CO_2$.

Unfortunately, our attempts to prepare crystals of compounds **1**–**4** suitable for a single crystal X-ray analysis, which could be positively to determine structure of the reaction products, were unsuccessful up to now.

### 3.4. Biological activity

Antitumor activity of all prepared complexes and the starting compounds, i.e. $CuCl_2·2H_2O$, $FeCl_3·6H_2O$, $HL_1$, $HL_2$ and $HL_3$, was determined. The data obtained from a LIVE/DEAD viability/cytotoxicity assay are presented in Table 5. All the tested complexes are shown to be potent growth inhibitors of different cancer cell lines, such as human malignant melanoma *G-361*, human osteogenic sarcoma *HOS*, human chronic myelogenous leukaemia *K-562* and human breast adenocarcinoma *MCF7*. The $IC_{50}$ values for $FeCl_3·6H_2O$ and $HL_1$ obtained on all used cell lines were found to be remarkably higher than those for the appropriate complexes. This indicates that the cytotoxic activity of the $HL_1$ ligand increases even more after the formation of the iron(III) complexes. Cell lines *G-361* and *MCF7* were the most sensitive to the assayed iron(III) complexes, displaying cytotoxicity with $IC_{50}$ in the range from 21 to 24 μM. Cell lines *HOS* and *K-562* were less sensitive in this case, with $IC_{50}$ ranging from 27 to 31 μM.

Surprisingly, formation of Cu(II) complexes had even stronger impact on antitumor activity of non-toxic compounds $HL_2$ and $HL_3$. The $IC_{50}$ found for prepared complexes **3** and **4** were in range from 17 to 39 μM, whereas the lowest $IC_{50}$ value determined for starting compounds, i.e. $HL_2$, $HL_3$ and $CuCl_2·2H_2O$, was 95 μM.

The inhibition of crude $p34^{cdc2}$ kinase by the most soluble complexes (**1**, **2**) was also estimated. The data obtained are shown in Table 6. As can be seen, very strong inhibitory effect was found for both studied compounds, indirectly pointing out about identical composition of complexes **1** and **2**. Unfortunately, the obtained results do not show any clear influence of complex formation on $p34^{cdc2}$ kinase inhibition, due to high activity of starting $HL_1$. However, found discrepancy that complex formation affect cytotoxicity of used ligands but not their ability to inhibit $p34^{cdc2}$ kinase can be explained by the finding that the cellular effect of cytotoxic 6-benzylaminopurine derivatives are not dependent only on their ability to inhibit CDKs and could be mediated by several other factors such as a decrease in the protein synthesis and/or glycolysis which in turn diminishes the ability of cancer cells to function [27].

Table 6
$IC_{50}$ values for tested compounds added to crude $p34^{cdc2}$ kinase

| Compound | $IC_{50}$ (μM) |
|---|---|
| 2-(3-Hydroxypropylamino)-6-(benzylamino)-9-isopropylpurine (Bohemin, $HL_1$) | 1.2 |
| **1** | 1.0 |
| **2** | 0.9 |

Enzyme activities were assayed as described in the Section 2, in the presence of increasing concentrations of tested compounds. $IC_{50}$ values were substracted from the dose-response curves.

## 4. Supplementary material

Crystallographic data for the structural analysis have been deposited with the Cambridge Crystallographic Data Centre, CCDC Nos. 156251 for compound $HL_2 \cdot 2H_2O$ and 156252 for compound $H^+HL_3$–Cl. Copies of this information may be obtained free of charge from The Director, CCDC, 12 Union Road, Cambridge, CB2 1EZ, UK (fax: +44-1223-336-033; e-mail: deposit@ccdc.cam.ac.uk or http://www.ccdc.cam.ac.uk).

## Acknowledgements

This research was supported by the Grant Agency of the Czech Republic (grants no. 203/00/0152 and 203/99/0067) and MSMT (grant no. MSM153100008).

## References

[1] Z. Trávníček, M. Maloň, Z. Šindelář, K. Doležal, J. Rolčík, V. Kryštof, M. Strnad, J. Marek, J. Inorg. Biochem. 84 (2001) 23.
[2] C. Mealli, F. Zanobini, J. Chem. Soc., Chem. Commun. (1982) 97.
[3] I. Søtofte, K. N, Acta Chem. Scan. A 35 (1981) 733.
[4] D.D. Swank, G.F. Needham, R. Willet, Inorg. Chem. 18 (1979) 761.
[5] J.C. Dayson, L.M. Engelhardt, P.C. Healy, C. Pakawatchai, A.H. White, Inorg. Chem. 24 (1985) 1950.
[6] J. Reedijk, Bioinorganic Catalysis, Marcel Dekker, New York, 1993.
[7] M. Rodriguez, A. Llobet, M. Corbella, Polyhedron 19 (2000) 2483.
[8] J.A. Kuhnle, G. Fuller, J. Corse, B.E. Mackey, Physiol. Plant 41 (1977) 14.
[9] E. König, Magnetic Properties of Coordination and Organometallic Transition Metal Compounds, Springer, Berlin, 1966.
[10] W.J. Geary, Coord. Chem. Rev. 7 (1971) 81.
[11] G.M. Sheldrick, Acta Crystallogr. A46 (1990) 467 SHELXS-97.
[12] G.M. Sheldrick, SHELXL-97, Program for crystal structure refinement, University of Göttingen, Germany, 1997.
[13] Z. Trávníček, M. Maloň, M. Biler, M. Hajdúch, P. Brož, K. Doležal, J. Holub, V. Kryštof, M. Strnad, Transition Met. Chem. 25 (2000) 265.
[14] A.B.P. Lever, Inorganic Electronic Spectroscopy, Elsevier, Amsterdam, 1968.
[15] (a) K.H. Reddy, P.S. Reddy, P.R. Babu, J. Inorg. Biochem. 77 (1999) 169;
(b) R.J. Parker, L- Spiccia, B. Moubaraki, K.S. Murray, B.W. Skelton, A.H. White, Inorg. Chim. Acta 302 (2000) 922.
[16] C.J. Pouchert, The Aldrich Library of Infrared Spectra (Edition III), Aldrich Chemical Co., INC, 1001 W. St. Paul. Ave., Milwaukee, Wisconsin, 53233, 1981.
[17] T. Fujita, T. Sakaguchi, Chem. Pharm. Bull. 25 (9) (1977) 2419.
[18] O. Kahn, Molecular Magnetism, Wiley-VCH Inc, New York, 1993.
[19] B.D. James, J. Liesegang, M. Balakova, W.M. Reiff, B.W. Skelton, A.H. White, Inorg. Chem. 34 (1995) 2054.
[20] L. Takacs, W.M. Reiff, B.D. James, Hyperfine Interact. 28 (1986) 693.
[21] D.Y. Jeter, D.J. Hodgson, W.E. Hatfield, Inorg. Chim. Acta 5 (1972) 257.
[22] D.J. Hodgson, Prog. Inorg. Chem. 19 (1975) 225.
[23] Ch. Chow, R.D. Willet, B.C. Gerstein, Inorg. Chem. 14 (1975) 205.
[24] M. Mégnamisi-Bélombé, M.A. Novotny, Inorg. Chem. 19 (1980) 2470.
[25] K. Emerson, A. Emad, R.W. Brookers, R.L. Martin, Inorg. Chem. 12 (1973) 978.
[26] M. Nardelli, J. Appl. Cryst. 28 (1995) 659.
[27] H. Kovářová, M. Hajdúch, G. Kořínková, P. Halada, S. Krupičková, A. Gouldsworthy, N. Zhelev, M. Strnad, Electrophoresis 21 (2000) 3757.